

# Combinatorial Constructions of Optical Orthogonal Codes for OCDMA Systems

Ivan B. Djordjevic and Bane Vasic, *Senior Member, IEEE*

**Abstract**—Two novel classes of optical orthogonal code (OOC) based on balanced incomplete block designs are proposed: OOC based on mutual orthogonal Latin squares/rectangles and the codes based on finite geometries. Both OOC families can be applied to synchronous and asynchronous incoherent optical CDMA, and are compatible with spectral-amplitude-coding (SAC), time-spreading encoding and fast frequency hopping schemes. Large flexibility in cross-correlation control makes those OOC families interesting candidates for applications that require a large number of users. Novel fiber Bragg grating decoding scheme for canceling the multi-user interference from SAC-signals with nonfixed in-phase cross-correlation is proposed as well.

**Index Terms**—Balanced incomplete block designs, finite geometries (FG), mutually orthogonal Latin squares/rectangles, optical CDMA (OCDMA), optical orthogonal codes (OOCs).

## I. INTRODUCTION

RECENTLY, several optical orthogonal codes (OOCs) families have been proposed [1]–[4], [6]–[9] for various optical CDMA (OCDMA) technologies: spectral-amplitude-coding (SAC) [2], [4]; time-spreading encoding [1], [3]; and fast frequency hopping [8].

The existing balanced detection schemes for SAC systems, [4], require unipolar sequences having fixed in-phase cross correlation. Hadamard code,  $m$ -sequence, modified quadratic congruence code (MQC) and modified frequency hopping (MFH) codes have been proposed for such applications [4], [7]. We propose a balanced detection fiber Bragg grating scheme (FBG), capable of canceling the multiuser interference (MUI) for SAC system employing unipolar codes with nonfixed in-phase cross correlations. The motivation for using such a detector is that the cardinality of the OOC, and therefore the number of simultaneous users, can be increased while maintaining the same performance.

We present two novel OOC classes based on mutually orthogonal Latin squares (MOLS) or mutually orthogonal Latin rectangles (MOLR) and finite geometries (FG), all the special cases of balanced incomplete block designs (BIBD). Three major advantages of proposed OOC families are: 1) large flexibility in choosing number of users (code size); 2) simplicity of construc-

tion; and 3) suitability to all important transmission technologies: spectral-amplitude-coding, time-spreading encoding and fast frequency hopping schemes. Spreading sequences of both MOLS and FG OOC families can be partitioned into “parallel” classes in such a way that the sequences from different parallel classes have zero cross correlation, which makes this class attractive for optical CDMA applications. For example, in fiber Bragg grating implementations the adjacent frequency bands are not ideally decoupled, and two sequences that involve adjacent bands should have zero cross correlation.

## II. OOC BASED ON MUTUALLY ORTHOGONAL LATIN RECTANGLES (MOLR)

An alternative and convenient way of representing OOCs is using combinatorial 2-designs [also referred to as balanced incomplete block designs (BIBDs)] [5]. A 2-design, denoted as  $2-(v, k, \lambda)$ , is a collection of  $k$ -subsets of a  $v$ -set  $V$  such that every 2-subset of  $V$  is contained in *exactly*  $\lambda$  blocks (with  $\lambda$  corresponding to the correlation constraint). In our constructions, MOLR and FG, every  $t$ -subset of  $V$  is contained in *no more* than  $\lambda$  blocks and is denoted by  $t-(v, k, \{0, \dots, \lambda\})$ , referred to as  $\lambda$ -configuration [5]. Latin squares/rectangles can be used to construct BIBD/ $\lambda$ -configurations.

A  $m \times k$  integer array with elements in  $V = \{0, 1, \dots, m\}$  is referred to as *Latin rectangle* (LR) if each of the elements occurs once in each row and once in each column. For two rectangles  $LR_1$  and  $LR_2$ , we define the *join*, an  $m \times k$  array whose  $(x, y)$ th entry is the pair  $\{LR_1(x, y), LR_2(x, y)\}$ . Two Latin rectangles are *orthogonal* if all entries in the join are distinct. The set of rectangles  $\{LR_1, LR_2, \dots, LR_n\}$  forms *mutually orthogonal* set if every two rectangles  $LR_i$  and  $LR_j$  are orthogonal.

To keep the exposition simple we restrict our attention to the MOLR construction of equal sizes (i.e., mutually orthogonal Latin squares, MOLS). Let  $k = m = p^l$  be a prime power ( $p$  is a prime,  $l \geq 1$ ;  $k$  and  $m$  are dimensions of a MOLS),  $\theta$  is a primitive element of a finite field  $\text{GF}(p^l)$ , and let  $\alpha_0 = 0, \alpha_1 = 1, \alpha_2 = \theta, \dots, \alpha_{p^l-1} = \theta^{p^l-2}$  be the elements of  $\text{GF}(p^l)$ . The Latin square (LS)  $LS_i$  ( $i = 1, 2, \dots, p^l - 1$ ) is designed by filling  $(x, y)$ th position by  $\alpha_x + \alpha_i \alpha_y$  ( $x, y = 0, 1, \dots, p^l - 1$ ). For example, the following two mutually orthogonal LS are obtained for  $\text{GF}(3)$ :

$$LS_1 = \begin{bmatrix} 1 & 2 & 3 \\ 2 & 3 & 1 \\ 3 & 1 & 2 \end{bmatrix} \text{ and } LS_2 = \begin{bmatrix} 1 & 3 & 2 \\ 2 & 1 & 3 \\ 3 & 2 & 1 \end{bmatrix}.$$

The elements in LSs are denoted by integers rather than Galois field elements ( $\alpha_0$  corresponds to 1,  $\alpha_1$  to 2, and  $\alpha_2$  to 3). By denoting the positions in LS from 1 to  $k^2 = 9$ , by reading off

Manuscript received November 4, 2003. The associate editor coordinating the review of this letter and approving it for publication was Prof. N. Ghani. This work is supported by the National Science Foundation under Grant ITR 0325979.

I. B. Djordjevic is with the Department of Electrical and Computer Engineering, University of Arizona, Tucson, AZ 85721 USA, on leave from the University of the West of England, Bristol BS16 1QY, U.K. (e-mail: ivan@ece.arizona.edu).

B. Vasic is with the Department of Electrical and Computer Engineering, University of Arizona, Tucson, AZ 85721 USA (e-mail: vasic@ece.arizona.edu).

Digital Object Identifier 10.1109/LCOMM.2004.831331

the positions of integers in  $LS_1$  and  $LS_2$ , the following matrix is created:

$$B = \begin{bmatrix} 1 & 6 & 8 \\ 2 & 4 & 9 \\ 3 & 5 & 7 \\ 1 & 5 & 9 \\ 3 & 4 & 8 \\ 2 & 6 & 7 \end{bmatrix}$$

Each row represents a codeword, with integers denoting the positions of ones in a codeword. Latin rectangle with different horizontal and vertical dimensions can be defined in a similar fashion.

The application of MOLR based OOCs to time-spreading systems and in spectral-amplitude-coding systems is straightforward, while the fast frequency hopping CDMA systems need the brief explanation. The labels in matrix  $B$  should be considered as different frequencies from a finite set of frequencies, and the integers assigned to a particular user define (ordered) set of frequencies assigned to him/her in the consecutive chip time slots. In the example above, there are 6 users, with maximum possible number of hits being 1.

### III. OOC BASED ON FINITE GEOMETRIES

The constructions proposed here are based on finite geometries [5] with projective geometries, affine geometries (AG), oval and unital designs all being special classes of a  $2-(v, k, \{0, 1\})$ -design, where  $v$  is the design set cardinality,  $k$  the size of the block in a design, and the overlapping between the blocks being 0 or 1. A one-to-one correspondence may be established between  $2-(v, k, \{0, 1\})$ -design and a OOC( $v, k, \{0, 1\}$ );  $v$  now representing the codeword length,  $k$  the codeword weight and maximum cross-correlation being 1; by assigning a *point-block matrix*  $A = (a_{ij})$  of dimensions  $v \times b$ , with elements determined by

$$a_{ij} = \begin{cases} 1, & \text{if } i\text{th point is contained in } j\text{th block} \\ 0, & \text{otherwise} \end{cases}$$

and the columns in the matrix representing different OOC codewords. The OOC cardinality is determined by  $b \approx v(v-1)/[k(k-1)]$ .

*Example:* The codewords of an OOC based on AG(2,3) are: {1,2,3}, {4,5,6}, {7,8,9}, {1,4,7}, {2,5,8}, {3,6,9}, {1,5,9}, {2,6,7}, {3,4,8}, {1,6,8}, {2,4,9}, {3,5,7}, where the labels denote the positions of ones within the codewords.

### IV. ENCODER/DECODER STRUCTURE FOR SAC SYSTEMS

If  $a = (a_1, a_2, \dots, a_\nu)$  and  $b = (b_1, b_2, \dots, b_\nu)$  are two different code sequences, then their in-phase cross correlation is defined as

$$R_{a,b} = \sum_{n=1}^{\nu} a_n b_n. \quad (1)$$

Sequences with nonfixed in-phase cross correlation do not satisfy the condition  $R_{\bar{a},b} = R_{a,b}$ , and the balanced detection

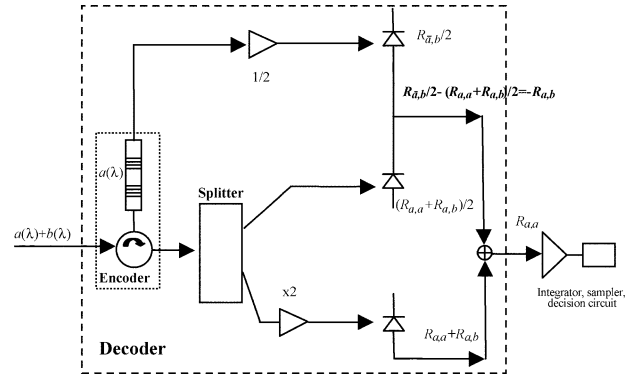


Fig. 1. Balanced MUI cancellation decoder scheme.

scheme in [4] cannot be applied. Those sequences satisfy the following relationship:

$$R_{\bar{a},b} + R_{a,b} = R_{b,b} \quad (2)$$

with  $R_{b,b} = b_1 + b_2 + \dots + b_\nu$  being the codeword weight.

We propose a novel fiber-Bragg grating (FBG) based balanced detection scheme that allows MUI cancellation when in-phase cross-correlation takes a value of 0 or 1. Such a detector allows us to relax the in-phase cross correlation constraint imposed on OOCs, and this leads to the construction of a new family of OOCs with larger cardinality. The proposed scheme therefore supports a larger number of simultaneous users, as it will be quantitatively shown in Section V. The transmitter and receiver structures based on FBGs are shown in Fig. 1.

When a bit "1" is sent, an optical pulse from a broadband source is launched into the encoder, while no optical pulse is launched for a data bit "0". The optical pulse passes through the linear FBG array in encoder and spectral components with the spectral distribution  $a(\lambda)$  are reflected. At the receiver, each grating is fixed according to the receiver's address. For proper decoding, the peak wavelengths are arranged in opposite order so that round-trip delays of different spectral components are compensated. The upper decoder branch, i.e. the balanced detection branch, is used to estimate the MUI, and its output is proportional to  $-R_{a,b}$ , while the lower branch is the signal-detection branch whose output is proportional to  $R_{a,a} + R_{a,b}$ . The signal values at all other points are indicated in Fig. 1. Therefore, the detector scheme shown in Fig. 1, completely cancels MUI.

### V. PERFORMANCE ANALYSIS

The minimum signal-to-noise ratio (SNR) of the spectral-amplitude-coding system employing any of the BIBD class of OOCs is calculated by using the method described in [4], [7], [9], and is given by the formula shown at bottom of the page, where  $R$  is the photodiode responsivity,  $P_{sr}$  is the effective power of a broadband source at the receiver,  $e$  is an electron charge,  $B$  is the electrical equivalent noise bandwidth of the receiver,  $k_B$  is Boltzmann's constant,  $T_r$  is the absolute temperature of receiver noise,  $R_L$  is the load resistance,  $\Delta f$

$$\text{SNR} = \frac{R^2 P_{sr}^2 k^2}{v^2} \frac{eBRP_{sr} \frac{k+(\lambda+1)(N-1)}{v} + \frac{BR^2 P_{sr}^2 kN}{2v^2 \Delta f} \left( \frac{N-1}{k-\lambda} + k + \lambda(N-1) \right) + \frac{4k_B T_r B}{R_L}}$$

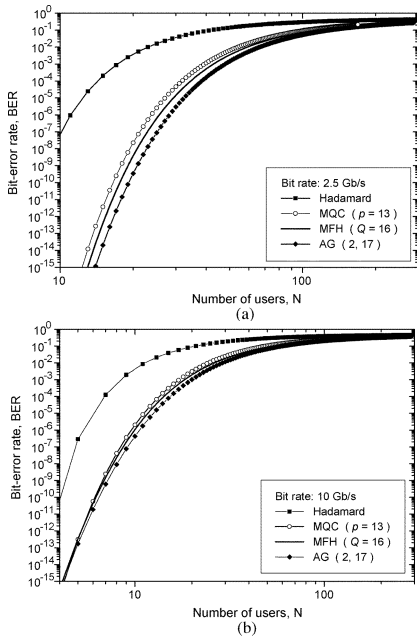


Fig. 2. AGs against MFH and MQC at: (a) 2.5 Gb/s and (b) 10 Gb/s ( $P_{sr} = -6$  dBm).

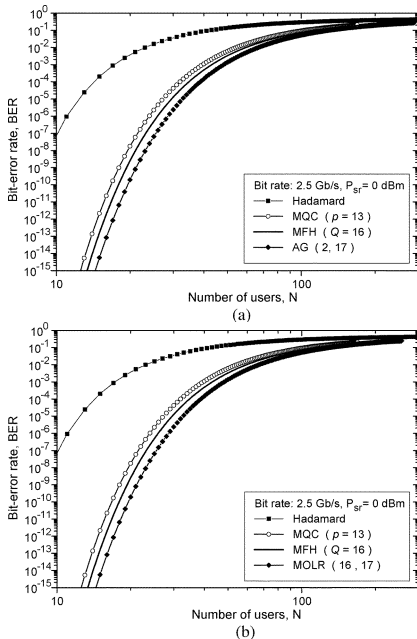


Fig. 3. BER versus number of active users for: (a) AG and (b) MOLR at 2.5 Gb/s and  $P_{sr} = 0$  dBm.

is the optical source bandwidth,  $N$  is the number of simultaneously active users, and  $v$ ,  $k$  and  $\lambda$  are the parameters of the BIBD. The phase induced intensity noise, the photodiode shot noise and the thermal noise are taken into account. The scheme capable of suppressing the MUI shown in Fig. 1 is considered. The bit-error rate (BER) can be calculated using the Gaussian approximation [2], [4]  $P_e = \text{erfc}(\sqrt{SNR}/8)/2$ .

The results of calculations are shown in Figs. 2 and 3, where the performance of MOLR and AG OOC families are compared against Hadamard codes [9], MQC [4], and MFH [2], in the presence of the phase induced intensity noise, the photodiode shot noise and the thermal noise. The system parameters are:  $\Delta\nu = 3.75$  THz, central wavelength 1550 nm,  $T_r = 300$  K,  $R_L = 1030 \Omega$ , and photodiode quantum efficiency 0.6. The bit rate per channel in Fig. 2(a) and Fig. 3 is 2.5 Gb/s ( $B =$

1.625 GHz), while that for Fig. 2(b) is 10 Gb/s. The effective power of a broadband source at the receiver is set to  $-6$  dBm for Fig. 2, and 0 dBm for Fig. 3 (reader is referred to [10] for the broadband light sources suitable for SAC applications). It is not difficult to see that the codes proposed here outperform MQC and MFH in terms of BER performance and cardinality. For example, the AG with  $m = 2$ ,  $p = 17$  and  $s = 1$  (the codeword weights are 17) supports 288 users, while MFH with  $Q = 16$  (codeword weights are 17) supports 256 users. For BER of  $10^{-9}$ , the system employing AG codes supports 21 2.5-Gb/s channels resulting in the total capacity of 52.5 Gb/s. Moreover, our code families have much larger flexibility in choosing the number of users, which is due to the fact that in our construction two or three parameters ( $p$  and  $l$  in MOLS,  $m$  and  $k$  in MOLR, and  $m$ ,  $p$  and  $s$  in AG) can be varied, as opposed to just one free parameter ( $p$  or  $Q$ ), in MQC or MFH. Finally, our OOC construction algorithms are very simple.

## VI. CONCLUSION

Two novel OOC classes based on mutually orthogonal Latin square/rectangles and finite geometries applicable to both synchronous and asynchronous incoherent optical CDMA for the following classes of systems: spectral-amplitude-coding, time-spreading encoding, and fast frequency hopping schemes are proposed. The proposed constructions offer a larger flexibility in choosing the number of users than previously reported OOC, and the construction algorithm is very simple. Novel balanced SAC decoder/receiver for MUI cancellation dealing with unequal in-phase cross correlation of optical orthogonal codes is also proposed.

Spreading sequences of both MOLS and FG OOC families can be partitioned into parallel classes, and the sequences from different parallel classes can be assigned to the adjacent frequency bands in the fiber Bragg grating implementations. In such a way sequences corresponding to adjacent (not ideally decoupled) frequency bands will have zero cross correlation.

## REFERENCES

- [1] J. A. Salehi, "Code division multiple-access techniques in optical fiber networks," *IEEE Trans. Commun.*, vol. 37, pp. 824–833, 1989.
- [2] Z. Wei and H. Ghafouri-Shiraz, "Proposal of a novel code for spectral amplitude-coding optical CDMA systems," *IEEE Photon. Technol. Lett.*, vol. 14, pp. 414–416, Mar. 2002.
- [3] F. R. K. Chung *et al.*, "Optical orthogonal codes: design, analysis, and applications," *IEEE Trans. Inform. Technol.*, vol. 35, pp. 595–604, May 1989.
- [4] Z. Wei *et al.*, "Modified quadratic congruence codes for fiber Bragg-grating-based spectral-amplitude-coding optical CDMA systems," *J. Lightwave Technol.*, vol. 19, pp. 1274–1281, Sept. 2001.
- [5] I. Anderson, *Combinatorial Designs: Construction Methods*. New York: Wiley, 1990.
- [6] K. Kamakura and I. Sasase, "A new modulation scheme using asymmetric error-correcting codes embedded in optical orthogonal codes for optical CDMA," *J. Lightwave Technol.*, vol. 19, pp. 1839–1850, Dec. 2001.
- [7] Z. Wei and H. Ghafouri-Shiraz, "Unipolar codes with ideal in-phase cross-correlation for spectral amplitude-coding optical CDMA systems," *IEEE Trans. Commun.*, vol. 50, pp. 1209–1212, Aug. 2002.
- [8] H. Fathallah, L. A. Rusch, and S. LaRochelle *et al.*, "Passive optical fast frequency-hop CDMA communication system," *J. Lightwave Technol.*, vol. 17, pp. 397–405, Mar. 1999.
- [9] E. D. J. Smith, R. J. Blaikie, and D. P. Taylor, "Performance enhancement of spectral-amplitude-coding optical CDMA using pulse-position modulation," *IEEE Trans. Commun.*, vol. 46, pp. 1176–1185, Sept. 1998.
- [10] Opto-Link Corporation Ltd.. (2002) ASE, LED Broadband Light Sources. [Online] <http://www.optolinkcorp.com/>